Supplementary Information

Air-permeable, multifunctional, dual-energy-driven MXene-decorated polymeric textile-based wearable heater with exceptional electrothermal and photothermal conversion performance

Xiaoya Liu[a#], Xiuxiu Jin[b#], Lei Li[a], Jianfeng Wang[a, c], Yanyu Yang[a], Yanxia Cao[a], Wanjie Wang[a]**

[a] College of Materials Science and Engineering, Henan Key Laboratory of Advanced Nylon Materials and Application, Zhengzhou University, Zhengzhou 450001, China

[b] Henan Provincial People's Hospital, Henan Eye Hospital, Henan Eye Institute, People's Hospital of Zhengzhou University, Zhengzhou, Henan, 450003, China

[c] The State Key Laboratory of Polymer Materials Engineering, Polymer Research, Institute of Sichuan University, Chengdu 610065, China

[#] XY Liu and XX Jin contribute equally to this work.

* To whom correspondence should be addresses. (Prof. Wang, Email: jfw@zzu.edu.cn, Fax:86-0371-67781590)
* To whom correspondence should be addresses. (Prof. Wang, Email: wwj@zzu.edu.cn, Fax: 86-0371-67781590)

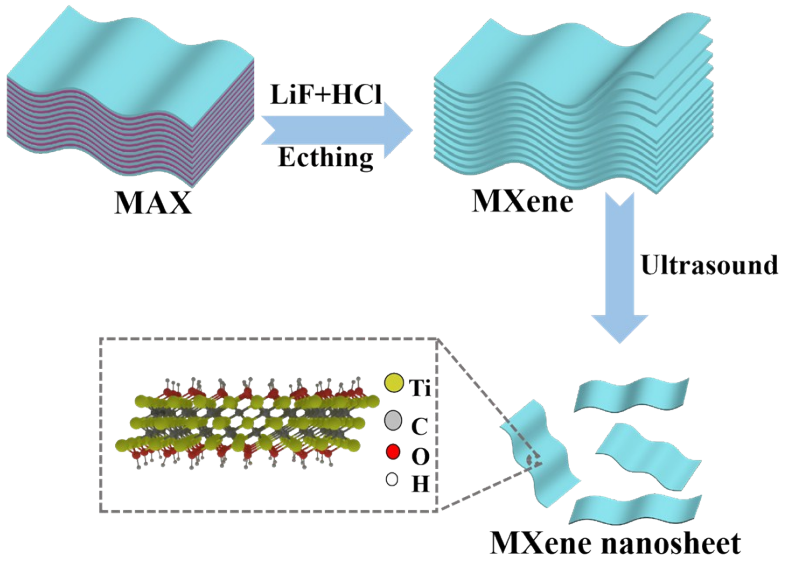

Fig. S1 Schematic illustration of the process for etching Ti_3C_2Tx MXene.

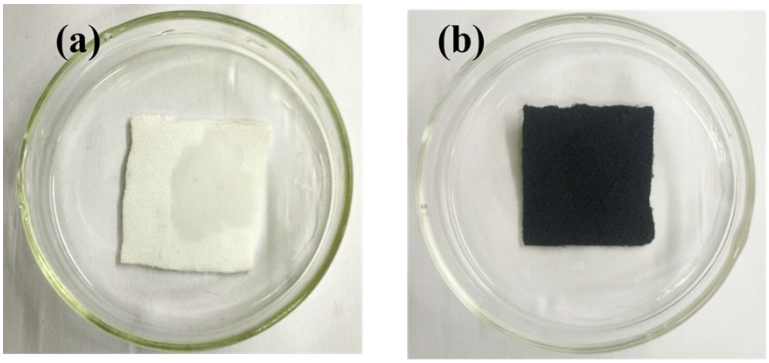

Fig. S2 Digital images of sample after sterilization: a) pristine textile and b) M-textile.

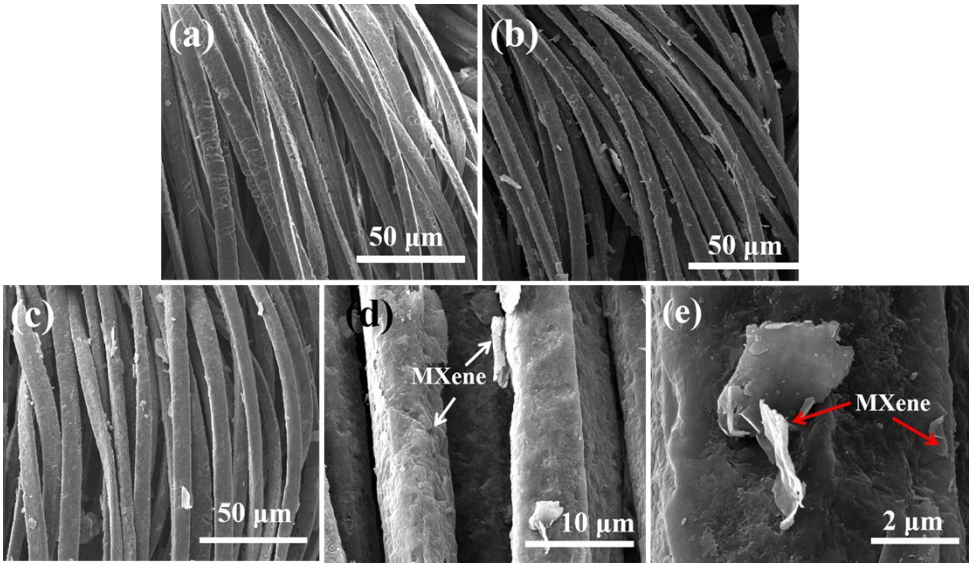

Fig. S3 SEM images of a) pristine textile, b) M-textile-17.3, c), d) and e) M-textile-4.7 at low and high magnification, respectively.

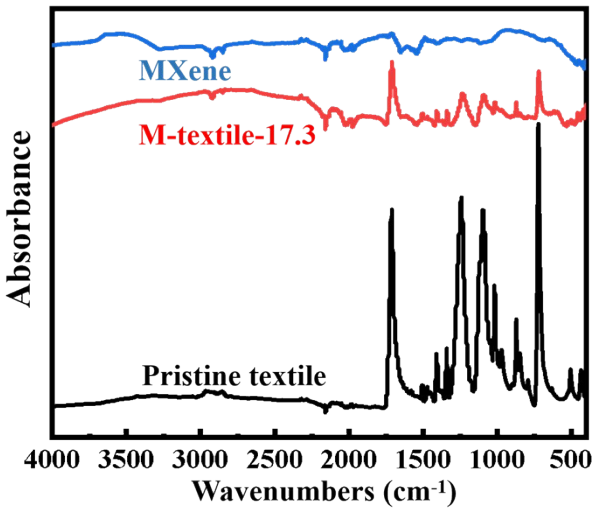

Fig. S4 ATR-IR spectra of the $Ti_3C_2T_x$, pristine textile, M-textile with different MXene content, respectively.

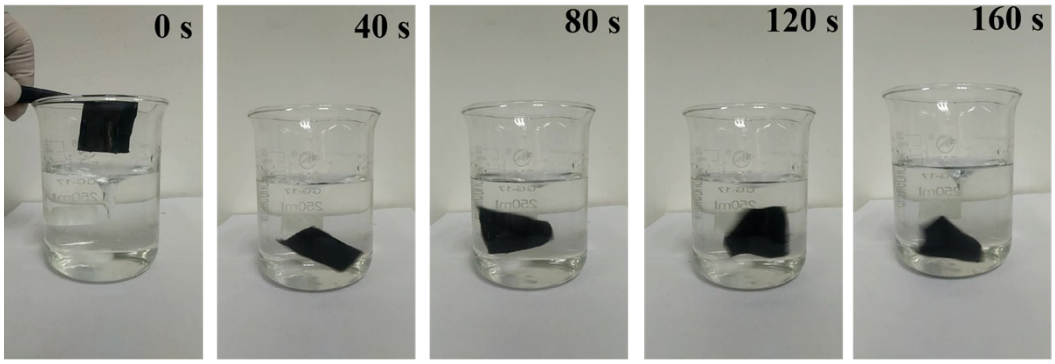

Fig. S5 Digital images of the mechanical washing process of M-textile-17.3.

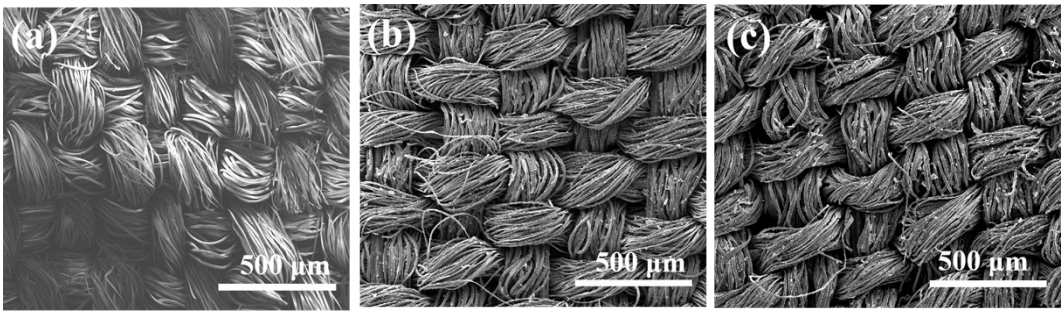

Fig. S6 SEM images of a) pristine textile, b) M-textile-4.7, and c) M-textile-17.3 at high magnification.

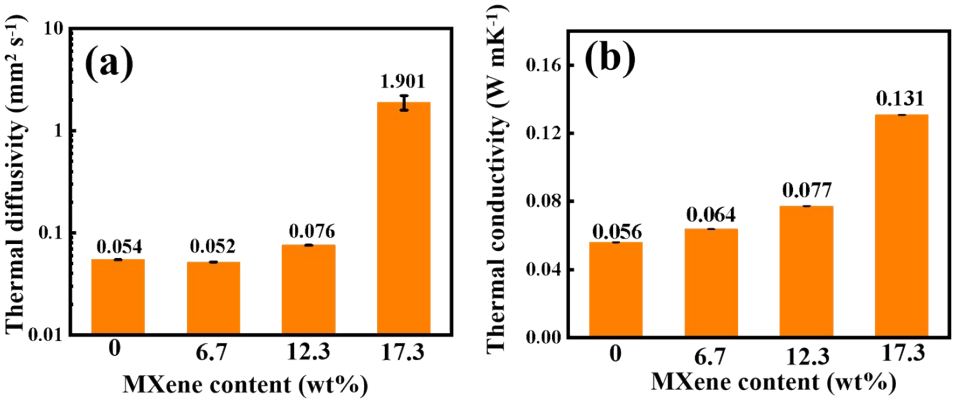

Fig. S7 a) Thermal diffusivity and b) thermal conductivity of pristine textile and M-textile with different MXene content, respectively.

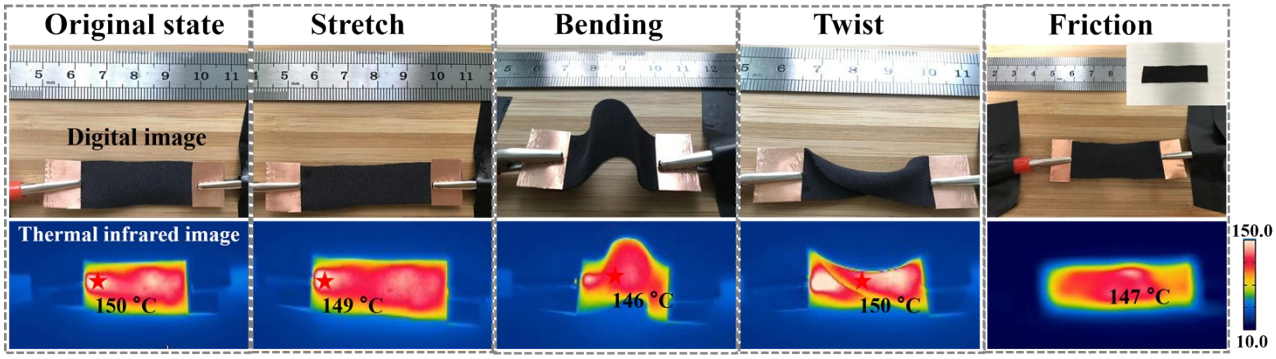

Fig. S8 Joule heating performance of M-textile-17.3 in the state of stretch (~120%), bending, twist or after one thousand time of friction on a paper.

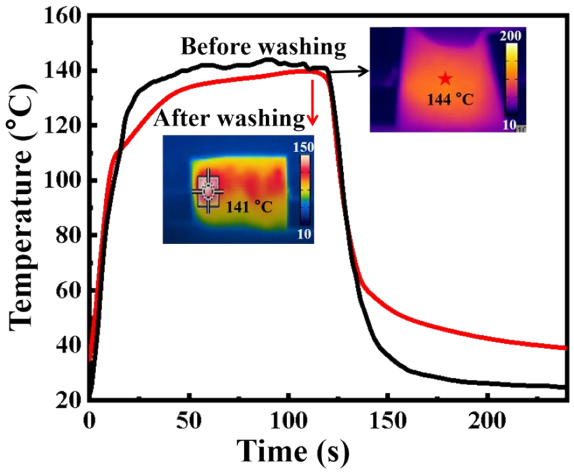

Fig. S9 Electrical heating performance (temperature rise curve and IR image at saturated temperature) of M-textile-17.3 textile at 3V before and after machine washing for 100 minutes.

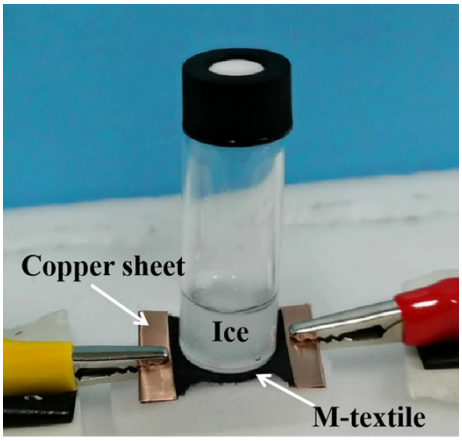

Fig. S10 Schematic diagram of electric heating deicing device based on M-textile.

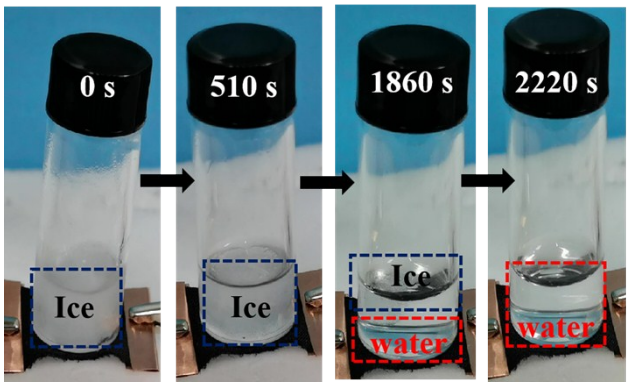

Fig. S11 Digital image of deicing process without applying voltage.

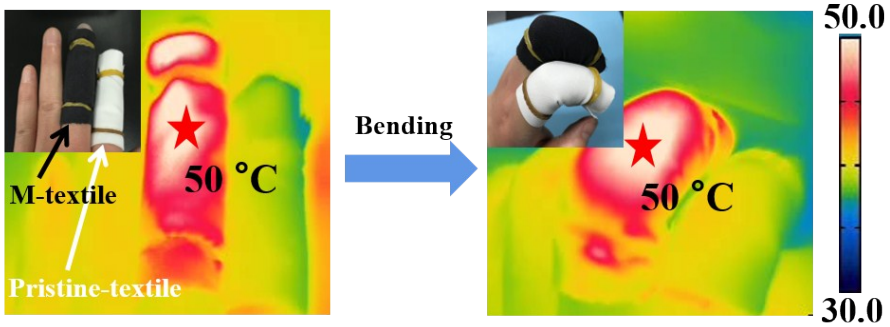

Fig. S12 IR images of straight and bended figures wrapped with M-textile and pristine textile during FIR light irradiating at a distance of 20 cm.

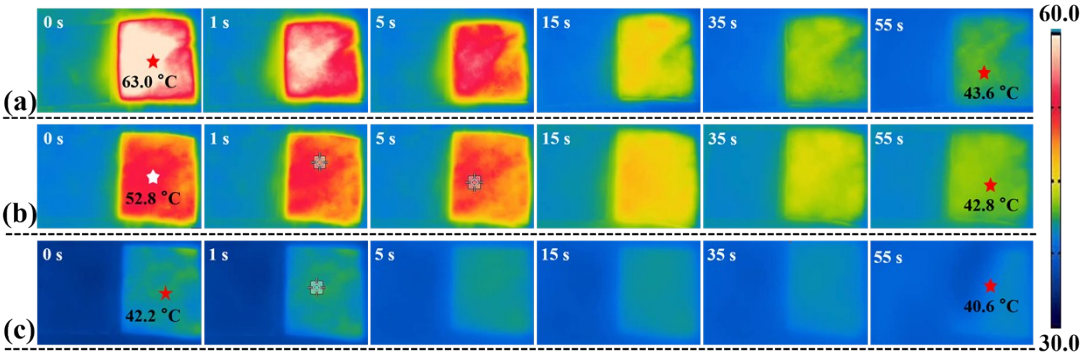

Fig. S13 IR images of the M-textile-17.3 after shading the sunlight at different time: a) 12 AM, b) 3 PM and c) 5 PM (May 2, Zhengzhou, China).

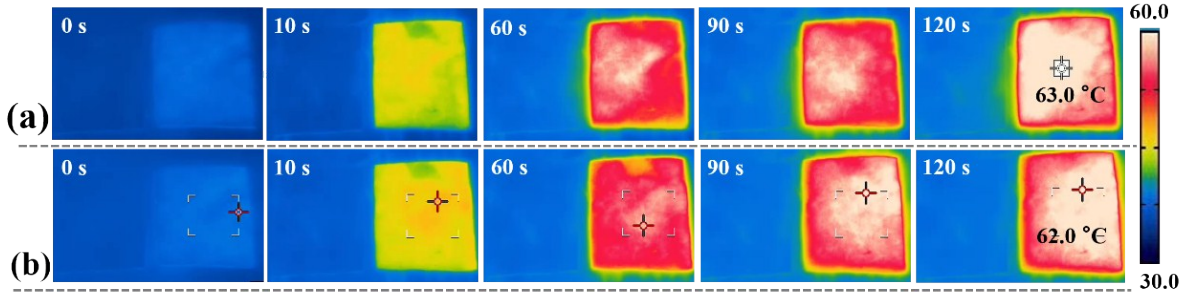

Fig. S14 IR images of a) 1st and b) 20th cyclic photothermal conversion performance of M-textile-17.3 including exposing to sunlight (2 min) and then shading sunlight (2 min) at 12 AM.

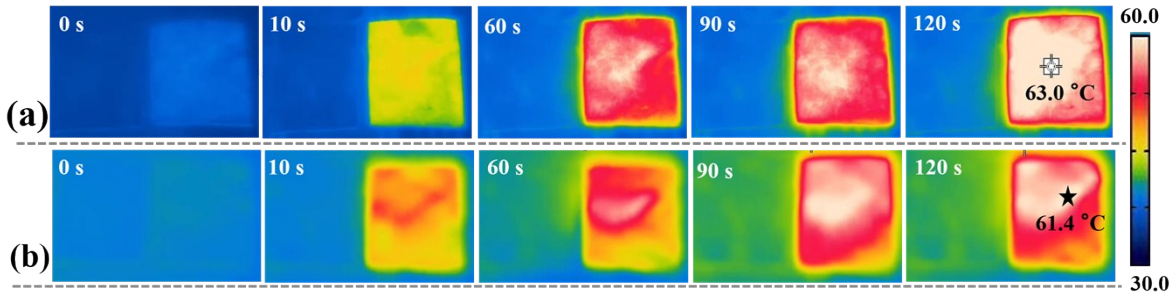

Fig. S15 IR images of the M-textile-17.3 exposed to sunlight at 12 AM a) before and b) after machine washing of 100 minutes.

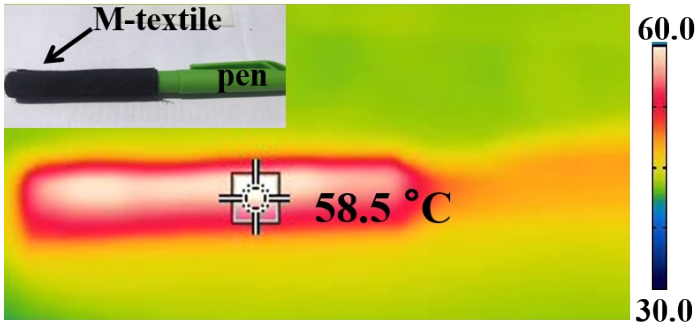

Fig. S16 IR images of a pen wrapped with M-textile-17.3 irradiated by sunlight at 12 AM.

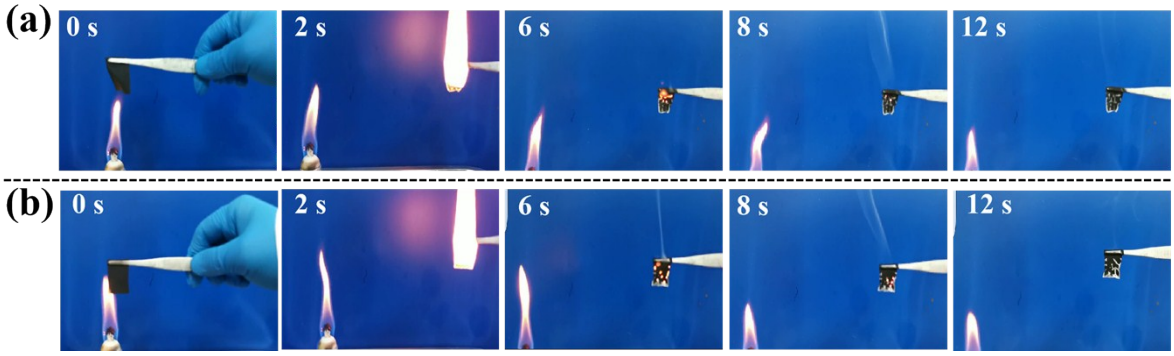

Fig. S17 Digital images of the combustion process at different time of a) M-textile-6.7 and b) M-textile-12.3.

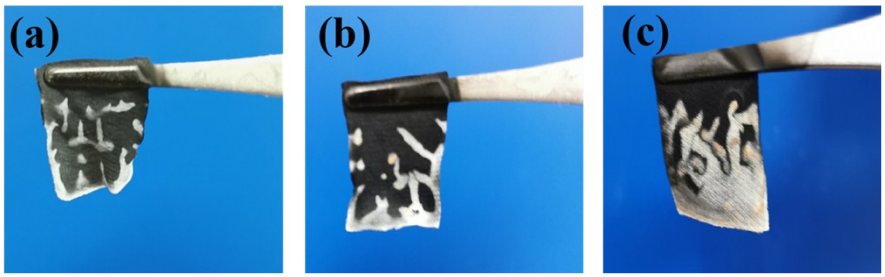

Fig. S18 Digital images of textiles after burning: a) M-textile-6.7, b) M-textile-12.3 and c) M-textile-17.3, respectively.

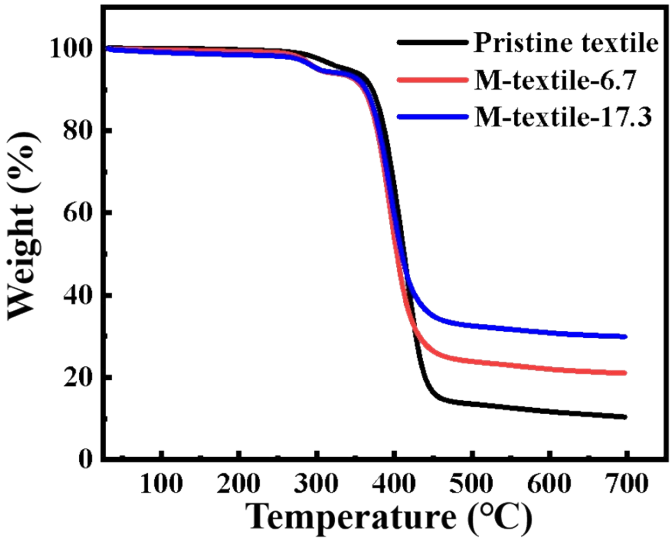

Fig. S19 TG curves of pristine textile and M-textile with different MXene content, respectively.

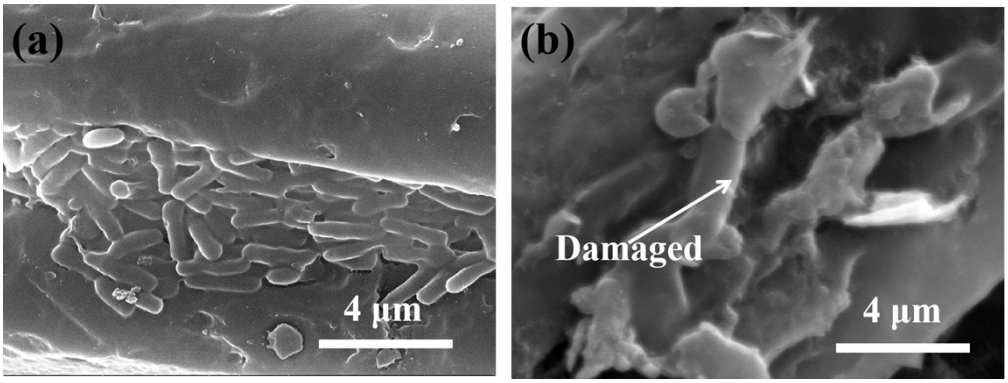

Fig. S20 SEM images of the B. subtilis colonies grown on a) of pristine textile and b) M-textile-4.7.

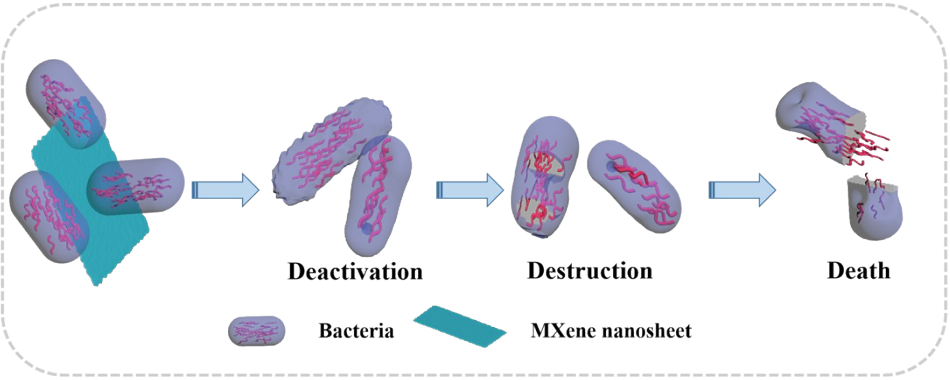

Fig. S21 The antibacterial mode of M-textile.

Table S1 Comparison of heating performance of the recently reported textile- and film-based wearable heaters. The references in this table correspond to those in the manuscript.

Heaters	Filler	Matrix	Sheet resistance (Ω sq^{-1})	Conductivity (S m^{-1})	Voltage (V)	Temperature (°C)	Ref.
Film-based	CuZr Metallic glasses	PDMS	4	/	7	180	2
	AgNW	PVA	26	/	5	74	3
	AgNW	Alumina	15	/	6	98	7
	CuNi MESH	PES	/	/	6	150	8
	Graphene		/	/	3.2	42	50
	Liquid-metal	PDMS	/	1.81×10^{6}	3.5	95.9	49
	CNT	TPU	/	142.6	6	65	44
	AgNW/ SWCNT	PDMS	/	/	5	87	45
	AgNW	Aramid Nanofibers	3.2	/	5	103.5	46
	CNT/FC	Aramid Nanofiber	/	230	10	113.5	47
	MWCNT		699	/	15	77	48
Textile-based	CuNW	PE Microfibers	2.5	/	3	57	1
	CNT Fiber		/	7.4×10^{5}	5	135	5
	PEDOT	Cotton	61	/	6	45	10
	MXene-PPy	PET	/	1000	4	79	20
	Conductive Weft-knitted Fabric		1.89	/	3.5	140	51
	CNT Fiber		/	110	1.5	47	52
	Silica NP/PDMS /AgNW	Cotton	2.8~4	/	0.5	34.1	53
	Ag/$Ni_{0.33}Co_{0.67}$ Se/PDMS /rGO	Woven Kevlar Fiber	/	/	2.1	79	54
	MXene	**PET**	**19.7**	**117**	**3.5**	**174**	**This work**